2014 IEEE/RSJ International Conference on
Intelligent Robots and Systems (IROS 2014)
September 14-18, 2014, Chicago, IL, USA

Fast Dual-Arm Manipulation Using Variable Admittance Control: Implementation and Experimental Results

Magnus Bjerkeng, Johannes Schrimpf, Torstein Myhre, and Kristin Y. Pettersen

Abstract— **This paper presents a control system for fast cooperative dual-arm manipulation of rigid objects with experimental results. The motivation for multi-arm manipulation comes from the wide range of applications. The possible tasks that can be performed by such a system greatly exceed those of a single manipulator system. The proposed system is flexible with respect to uncertainties in object size. Moreover, it allows for physical human interaction through force/torque sensing. This is especially beneficial in industrial cases where humans and robots work on the same production line. One main goal of this paper is to bridge the gap between current research regarding dual-arm manipulation and the implementation possibilities on current industrial robots and widely available standard hardware.**

I. Introduction

The use of multiple manipulators is considered as a natural solution for many manipulation and assembly tasks. One of the reasons for this is that a two-arm system is anthropomorphic since humans have two arms. Humans therefore have an intuitive understanding of bimanual manipulation, such that actions carried out by a two-arm system are easier to relate to, [1].

Automation is expected to become more prevalent in the industry, and processes which traditionally have been carried out by humans are considered for robotization. The work cells in question have been designed for humans. Robotic systems with human-like features can relieve the need for major redesign of the existing work cells during the automation process.

For manipulation tasks like pick-and-place operations, single arm systems are restricted by the gripper that is used. Specialized interchangeable grippers are needed to cope with objects varying in size and shape. However, two robotic arms can carry objects between them that are of greater size and weight than what is possible with single arm. This is even possible without customized grippers [2].

The use of two-arm robot system are as old as robot manipulator themselves. Early applications are reported as early as the 1940s and 50s where two manipulators were independently teleoperated for handling radioactive materials, [3]. In the late 50s and 60s dual arm systems were used in subsea exploration [4], and more recently for anthropomorphic teleoperation at NASA [5]. For a survey of previous and ongoing works in two-arm manipulation see [6].

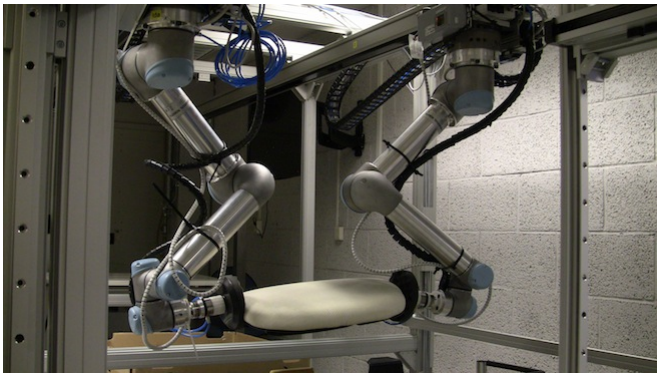

Fig. 1: The demonstrator cell including two linear axes and two robots with force sensors mounted on the tool flange.

The control problem of cooperative manipulation falls within the force/motion framework. Several strategies for controlling the motion of the manipulated objects as well as the different forces involved have been presented: In [7] and [8] a decentralized control architecture is considered for motion tracking and control of internal forces. Controllers based on the synchronization framework have been presented in [9] and [10] for cooperative assembly tasks. In this framework individual robot motions are generated to minimize a collective synchronization error. Control schemes based on Fuzzy logic for cooperative manipulation is explored in e.g. [11] and [12]. Impedance control has been exploited for controlling environmental interaction forces in [13], and internal grasping forces in [14]. These two approaches are combined using a centralized architecture in [15] to achieve object motion control as well as bounded internal and external forces.

One challenge involved in implementing multi-robot cooperative handling schemes on industrial manipulators is restrictive control interfaces. Typically joint torque access is unavailable, and higher-level control methods are used instead.

This paper proposes a centralized architecture for fast cooperative control of a multi-robot system. The controller handles both internal and external forces, and is based on the control method proposed in [15].

A velocity-level on-line trajectory generator is used, and no torque access is needed. In particular, a centralized variable admittance-based control architecture for cooperative handling for redundant industrial manipulators is proposed.

M. Bjerkeng is with Applied Cybernetics, SINTEF ICT, Trondheim, Norway. Magnus.Bjerkeng@sintef.no

J. Schrimpf, is with the Department of Engineering Cybernetics, Norwegian University of Science and Technology, Trondheim, Norway.

K. Y. Pettersen is with the Center for Autonomous Marine Operations and Systems, at the Department of Engineering Cybernetics, Norwegian University of Science and Technology, Trondheim, Norway.

T. Myhre is with the Department of Production and Quality Engineering, Norwegian University of Science and Technology, Trondheim, Norway

The presented design has a heavy focus on simplicity of implementation, and considers 1st order dynamics with isotropic admittance behavior for both internal and external forces.

The contributions of this paper are as follows.

- A centralized variable admittance force/position control scheme for two cooperating redundant industrial manipulators is presented.
- Variable admittance control is proposed as a solution for achieving fast environmental interaction during tracking in a safe and intuitive manner.
- Special emphasis is placed on simplicity of implementation, robustness and applicability for standard industrial robots compared to previous works that use less restrictive research platforms.
- Experiments which include motion tracking during compliant cooperative object handling and human interaction are presented.
- A comparison between the presented experiment and data from related experiments found in the literature is given. An emphasis is placed on execution speed.

One main goal is to bridge the gap between research currently being carried out for dual-arm manipulation, and the implementation possibilities on current industrial robots and widely available standard hardware. The controller is implemented in Python/C++ using ROS[1]. The implementation is modular, and is easily extensible to other industrial manipulator interfaces based on position or velocity control.

The paper is organized as follows: Section II presents the robot kinematics and grip modelling. Section III presents the proposed control method. In Section IV an overview of the hardware and software implementation is given. Experimental results are presented in Section V, followed by a comparison to previous experiments found in the literature. Conclusions and future work are presented in VI.

II. Modeling

This section presents the notation used, the robot's kinematic model, and the grip modeling. Consider two serial link industrial manipulators which cooperatively grasp an object. The joint positions of the two robots are denoted $\boldsymbol{q}_{k=1,2} \in \mathbb{R}^n$. Both manipulators are identical with 7 joints, ($n = 7$) which results in fully redundant manipulators following the definition in [16].

The forward kinematics of each robot is given by $\boldsymbol{x}(\boldsymbol{q}_k), \mathbf{R}(\boldsymbol{q}_k)$ where $\boldsymbol{x}(\boldsymbol{q}_k) \in \mathbb{R}^3$ denotes its position relative to the workcell base frame. $\mathbf{R}(\boldsymbol{q}_k) = \mathbf{R}_k \in SO(3)$ is a rotation matrix describing the orientation of the end-effector in the same base frame. $\boldsymbol{Q}_k$ denotes the unit quaternion corresponding to the rotation matrix $\mathbf{R}_k$. The manipulator Jacobian for each robot is given by $\mathbf{J}_k = \mathbf{J}(\boldsymbol{q}_k) \in \mathbb{R}^{6\times n}$ such that

$$\boldsymbol{\xi}_k = \begin{bmatrix} \dot{\boldsymbol{x}}_k \\ \boldsymbol{\omega}_k \end{bmatrix} = \mathbf{J}(\boldsymbol{q}_k)\dot{\boldsymbol{q}}_k \tag{1}$$

[1] www.ros.org

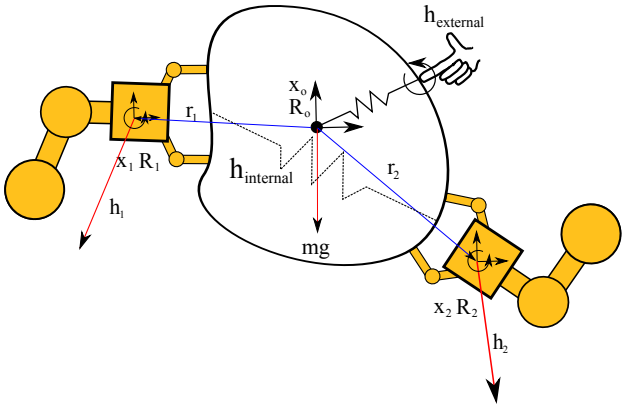

Fig. 2: The different coordinate systems and forces which are used to model the cooperative handling task.

where $\boldsymbol{\xi}_k$ denotes the twist of robot k, with linear velocity $\dot{\boldsymbol{x}}_k$ and angular velocity $\boldsymbol{\omega}_k$. All these quantities follow standard notation in robot kinematics [17].

Let the frame $\{\boldsymbol{x}_o, \mathbf{R}_o\}$ denote the nominal coordinate system attached to the grasped object. It is assumed that $\boldsymbol{x}_o$ is located at center of mass of the object, and the object is grasped tightly enough to avoid slipping. Each robot can exert a wrench $\boldsymbol{h}_k = [\boldsymbol{f}_k^T, \boldsymbol{\tau}_k^T]^T$ on the object at their grasping point. We will without loss of generality assume that the kinematics of the two manipulators are constructed such that $\mathbf{R}_1 = \mathbf{R}_2 = \mathbf{R}_o$ at a nominal grasp. An illustration is seen in Fig. 2

The following grasp matrix $\mathbf{W} \in \mathbb{R}^{6\times 12}$ maps the forces exerted on the object by the robots to the external wrench $\boldsymbol{h}_e = [\boldsymbol{f}_e^T, \boldsymbol{\tau}_e^T]$, which contributes to the motion of the object

$$\boldsymbol{h}_e = \begin{bmatrix} \mathbf{I}_{3\times3} & \mathbf{O}_{3\times3} & \mathbf{I}_{3\times3} & \mathbf{O}_{3\times3} \\ \mathbf{S}(\boldsymbol{r}_1) & \mathbf{I}_{3\times3} & \mathbf{S}(\boldsymbol{r}_2) & \mathbf{I}_{3\times3} \end{bmatrix} \begin{bmatrix} \boldsymbol{h}_1 \\ \boldsymbol{h}_2 \end{bmatrix} = \mathbf{W}\boldsymbol{h}. \tag{2}$$

In (2), $\mathbf{O}_{k\times m} \in \mathbb{R}^{k\times m}$ denotes the $k \times m$ dimensional zero-matrix, $\mathbf{I}_{k\times k} \in \mathbb{R}^{k\times k}$ denotes the identity matrix, and $\mathbf{S}(\boldsymbol{x}) : \mathbb{R}^3 \mapsto \mathbb{R}^{3\times3}$ denotes the skew-symmetric matrix operator performing the cross product with $\boldsymbol{x}$. The vectors $\boldsymbol{r}_k^o \in \mathbb{R}^3$ are the *virtual sticks* which are the vectors from an object-fixed point $\boldsymbol{x}_o$, to the kth end effector decomposed in the object-attached frame [18]. The inverse solution to (2) is given by

$$\boldsymbol{h} = \mathbf{W}^\dagger \boldsymbol{h}_e + \mathbf{V}\boldsymbol{h}_i = \boldsymbol{h}_E + \boldsymbol{h}_I \tag{3}$$

where the pseudoinverse $\mathbf{W}^\dagger$ is the *no-squeeze* pseudoinverse and the columns of $\mathbf{V}$ span the null-space of $\mathbf{W}$ e.g. $\mathbf{V} = \mathbf{I}_{12\times12} - \mathbf{W}^\dagger\mathbf{W}$. The no-squeeze pseudoinverse given by

$$\mathbf{W}^\dagger = \frac{1}{2}\begin{bmatrix} \mathbf{I}_{3\times3} & \mathbf{O}_{3\times3} \\ -\mathbf{S}(\boldsymbol{r}_1) & \mathbf{I}_{3\times3} \\ \mathbf{I}_{3\times3} & \mathbf{O}_{3\times3} \\ -\mathbf{S}(\boldsymbol{r}_2) & \mathbf{I}_{3\times3} \end{bmatrix} \tag{4}$$

is used as opposed to the common Moore-Penrose pseudoin-

verse. This is necessary to avoid unwanted internal forces [19]. The internal wrenches produced by the end-effectors, which contribute to internal stresses are given by

$$\boldsymbol{h}_I = \begin{bmatrix} \boldsymbol{h}_{I_1} \\ \boldsymbol{h}_{I_2} \end{bmatrix} = \mathbf{V}\mathbf{V}^{\dagger}\boldsymbol{h}. \tag{5}$$

The geometry of the grasp can be summarized by the following constraints on the end-effector motions.

$$\begin{aligned} \boldsymbol{x}_k &= \boldsymbol{x}_o + \mathbf{R}_o \boldsymbol{r}_k^o \\ \mathbf{R}_o &= \mathbf{R}_k \\ \dot{\boldsymbol{x}}_k &= \dot{\boldsymbol{x}}_o + S(\boldsymbol{\omega}_o)\mathbf{R}_o \boldsymbol{r}_k^o \\ \boldsymbol{\omega}_o &= \boldsymbol{\omega}_k \end{aligned} \tag{6}$$

III. Controller Overview

This section presents an overview of the control method used for generating the motion of the robots during cooperative handling. The presented controller is based on the controller developed in [15]. The main differences between the controllers are the following:

1) The dynamics used for the high-level trajectory generation is here considered as 1st order in time, which results in a velocity generator. The reason for this choice is to keep the system as simple and computationally efficient as possible. However, note that large accelerations will result in force measurement errors.
2) Redundancy resolution is implemented in the velocity generator, see [20]. The classical resolved redundancy control scheme is used where the extra degree of freedom is chosen to achieve minimal joint velocity for the two robots individually.
3) We consider here a PI force controller for the internal forces. This integral action in the controller allows for tight gripping during the motion of the object even when the dimensions of the objects are uncertain.
4) A variable admittance scheme is introduced in order to allow for human interaction during object motion tracking. This feature is crucial for operation at higher speeds.

A. Reference Object Dynamics

In this section the reference object dynamics are presented. It is assumed that a desired position and velocity is available for the object. The control routine seeks to comply with external forces, while tracking a user-defined trajectory. A 1st order in time variable admittance scheme is adopted for the position and orientation convergence of the object. The detection of external forces slows down the object convergence rates, effectively making the object more compliant. This feature allows for human interaction in an intuitive manner, and also allows for faster motion tracking.

Let the vector $\boldsymbol{x}_{\text{des}}(t)$ denote the desired object position given in an inertial frame at time t, and the quaternion $\boldsymbol{Q}_{\text{des}}(t)$ corresponding to the rotation matrix $\mathbf{R}_{\text{des}}(t)$ denote the desired orientation of the object. The desired linear and angular velocities of the object are denoted $\dot{\boldsymbol{x}}_{\text{des}}$ and $\boldsymbol{\omega}_{\text{des}}$.

The dynamics of the object which should comply with external forces applied to it, is a 1st order variant of the external impedance scheme developed in [13]. The object's velocity is given by

$$\dot{\boldsymbol{x}}_o = \alpha\big[-k_p \arctan(\boldsymbol{x}_o - \boldsymbol{x}_{\text{des}}) + \dot{\boldsymbol{x}}_{\text{des}}\big] + k_{E_f}(\boldsymbol{f}_e - \boldsymbol{g}\hat{m}) \tag{7}$$

$$\boldsymbol{\omega}_o = \alpha\big[k_o \tilde{Q}_v + \boldsymbol{\omega}_{\text{des}}\big] + k_{E_\tau}\boldsymbol{\tau}_e \tag{8}$$

where the trigonometric function $\arctan$ is used as a sigmoid velocity profile in order to achieve an upper velocity bound and $k_p, k_o > 0$ are convergence gains. The external force $\boldsymbol{f}_e$ and torque $\boldsymbol{\tau}_e$ are given by Eq. (2) and are computed using measurements from the wrist-mounted force/torque sensors. The external admittance gains $k_{E_f}, k_{E_\tau} > 0$ define how the external forces influence the object velocity. The external force due to gravity $m\boldsymbol{g}$ is canceled, assuming that an estimate of the object mass is known. Orientation convergence is achieved using classical quaternion feedback [21]. In (8), $\tilde{Q}_v$ is the vector part of the unit quaternion extracted from the matrix product $\mathbf{R}_o^T\mathbf{R}_{\text{des}}$. The Eqs. (7)-(8) are numerically integrated on-line to produce a reference position and velocity for the object.

The factor α is used to tune the tracking convergence of the object. In the case where $\alpha = 0$, it is seen that controller (7)-(8) is reduced to a pure compliance controller, complying with external forces. A 1st order hysteresis dynamical response of α is designed as

$$\dot{\alpha} = \begin{cases} -k_{\text{speed down}}\alpha, & \text{if } \left\| \mathbf{D}\left(\boldsymbol{h}_E - \begin{bmatrix} \hat{m}\boldsymbol{g} \\ \mathbf{0}_{3\times 1} \end{bmatrix}\right) \right\| > \epsilon \\ -k_{\text{speed up}}(\alpha - 1) & \text{else} \end{cases}. \tag{9}$$

The positive gains $k_{\text{speed down}}, k_{\text{speed up}}$ define how fast the object should lower its speed due to external interaction, and regain its assigned speed when no external force is measured. Typically, it is desirable that the object should speed down more rapidly than it should speed up. With this behavior, the robots will not apply high forces to a human operator. The positive-definite weighting matrix $\mathbf{D}$ and the lower threshold ϵ tune at what magnitude of external forces and torques a speed-change is triggered. Replanning of $\boldsymbol{x}_{\text{des}}(t), \mathbf{R}_{\text{des}}(t)$ may be necessary if external interaction pushes the object far from its originally planned trajectory.

B. End-Effector Dynamics

This section presents the end-effector velocity generation for the robot manipulators during the cooperative object handling. The end-effector velocities are calculated using the object reference position and velocity, as well as force measurements. Each manipulator has two main motion components; the grip constrained motions which should realize (7)-(8), and motion component which seeks to keep a firm grasp on the object and bound the internal forces. To control the internal forces, a 1st order implementation of the internal impedance scheme from [14] is used with added integral gain. In accordance with the gripping constrains (6), the

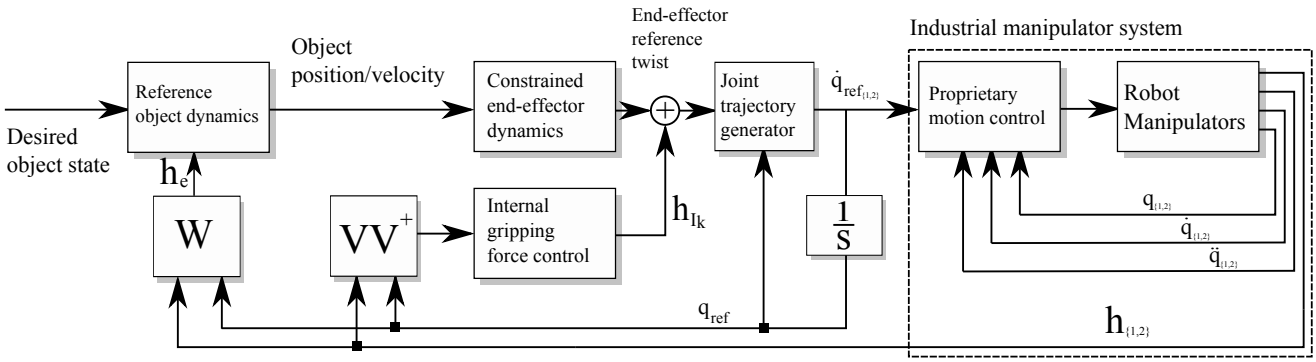

Fig. 3: The control structure.

following end-effector velocities are assigned,

$$\dot{\boldsymbol{x}}_k = \dot{\boldsymbol{x}}_o + S(\boldsymbol{\omega}_o)\mathbf{R}_o \boldsymbol{r}_k + k_{f_p}\tilde{\boldsymbol{f}}_{I_k} + k_{f_i}\mathbf{R}_o \int_0^t \tilde{\boldsymbol{f}}^o_{I_k} dt \quad (10)$$

$$\boldsymbol{\omega}_k = \boldsymbol{\omega}_o + k_{\tau_p}\tilde{\boldsymbol{\tau}}_{I_k} + k_{\tau_i}\mathbf{R}_o \int_0^t \tilde{\boldsymbol{\tau}}^o_{I_k} dt, \quad (11)$$

where the error between the measured wrench and a desired gripping wrench $\boldsymbol{h}_{I_{\text{des}}}$ is given by

$$\begin{bmatrix} \tilde{\boldsymbol{f}}_{I_k} \\ \tilde{\boldsymbol{\tau}}_{I_k} \end{bmatrix} = \boldsymbol{h}_{I_k} - \boldsymbol{h}_{I_{\text{des}}}. \quad (12)$$

The gripping force controller is a PI controller with appropriate positive gains. The integral term is desirable since the shape of the object may be uncertain. One example which shows the integral action the following: The robots grip a box which is assumed to have straight sides. In reality the sides are slightly angled, or the object is somewhat smaller or larger than what is assumed. The integral action in the controller will adjust the grip to correct for the resulting force error, using the measured end-effector torques. In the case of a too small object, the integral action will build up to tighten the grip.

The internal forces are calculated using Eq. (5). The end-effector velocities defined by Eqs. (10)-(11) are given as inputs to the joint trajectory generator presented below.

C. Joint Trajectory Generator

The low-level joint trajectory generator is presented in this section. There are two identical trajectory generators, one for each robot, which operate independently of one another. The trajectory generators take a twist $\boldsymbol{\xi} = [\dot{\boldsymbol{x}}^T_{\text{ref}}, \boldsymbol{\omega}_{\text{ref}}]^T$ as input, and calculate the corresponding joint velocities $\dot{\boldsymbol{q}}_{\text{ref}}$ using the 1st order in time resolved motion rate control scheme presented in [22]

$$\dot{\boldsymbol{q}}_{\text{ref}} = \mathbf{J}^{\dagger}\boldsymbol{\xi}. \quad (13)$$

The joint trajectories given by integrating (13) seek to achieve the prescribed end-effector twist while optimizing the magnitude of $\dot{\boldsymbol{q}}$. The reference velocity $\dot{\boldsymbol{q}}_{\text{ref}}$ is sent to the low-level joint controller. It is assumed that the joint servo controllers, which are produced by the industrial robot manufacturer, function nominally such that

$$\boldsymbol{q} \approx \boldsymbol{q}_{\text{ref}}, \quad \dot{\boldsymbol{q}} \approx \dot{\boldsymbol{q}}_{\text{ref}}. \quad (14)$$

IV. System Description

This section describes the hardware and software layout of the demonstrator workcell. The demonstrator workcell is seen in Fig. 1.

A. Robots

Two UR-6-85-5-A industrial manipulators from Universal Robots were used. The robots ship with a controller cabinet including a servo controller board and a PC running the high-level controller software on a Debian GNU/Linux operating system. The controller includes different interfaces for external controllers.

The most commonly used interface for controlling the robot from an external PC is the *Secondary Client Interface* that allows for sending commands via TCP. These commands are high-level commands, for example commands to move the robot with a given tool velocity, or towards a target position. This interface is very convenient for a wide range of industrial applications, but has its limitations when real-time control is required.

Since the concepts presented in this paper make use of force-based sensor feedback control, another interface was used for the real-time control parts of the system. Due to the Linux-based control platform and the availability of a library to directly access the low-level controller, it is possible to compile custom controllers on the robot controller hardware. By doing this, it is possible to obtain joint position and velocity measurements as well as command new joint positions, velocities and accelerations with a frequency of 125 Hz. A router application was programmed that makes it possible to connect to this interface from an external PC via Ethernet/UDP.

B. Linear Axes

Two 3 m Festo EGC-TB-KF linear axes were installed in the demonstrator cell to extend the working area of the robots. Using these axes, the two robots can be seen as 7-DOF industrial manipulators. The axis controllers can be

accessed from external hardware using a CAN connection. A CANUSB dongle was installed for each of the axes to send initialization commands, read the current positions, and send position commands. The communication frequency is set to 1 kHz. A driver was implemented as a C++ library to provide access to the axis system for other applications.

C. Trajectory Generator PC

A standard PC running Ubuntu Linux was used for trajectory generation. It is connected to the robots via Ethernet and to the linear axes via a CANUSB dongle. Since the low-level interface of the robot does not support movements in task space, only in joint space, an external trajectory generator was installed on the PC. The used trajectory generator was written in Python using the Orocos KDL library. Implementation details can be found in [23]. A tool trajectory generator is used to calculate the joint updates from the desired tool velocity in real-time, implementing (13). While the trajectory generator is synchronized with the robot system and thus runs with a frequency of 125 Hz, the tool velocity can be updated asynchronously.

D. Force Sensors

To make it possible for the robots to interact with their environment, force sensors were installed on the tool flanges of the two robots. The sensors are ATI Mini45s with Net F/T sensor interface, connected to the controller PC via Ethernet. The update rate was set to 1 kHz in the ROS-based driver on the PC.

E. Control PC

The control PC is a standard PC running Ubuntu Linux. ROS was installed to provide a communication platform for the different nodes. ROS is a set of libraries and tools for development of robot applications. It provides facilities for communication including support for messages and services that are similar to remote procedure calls in other communication middlewares. ROS also includes utilities for logging, debugging and data visualization. The controller PC runs the drivers for the force sensors and the ROS-based controller node that is programmed in Python.

The choice of Python as main language for the control application despite the lack of hard real-time functionality is due to the decision to develop a system that allows for fast prototyping rather than industrial stability. Computationally intensive parts of the programs were based on C/C++ libraries that can be included in Python. Regarding sensor-based robot control using Python, previous work has shown that the main cause of delays in the used ROS-based sensor/robot system is due to asynchronous loops and delays in the robot system that cannot be influenced rather than communication delay and computation time, [24].

V. EXPERIMENTS

This section presents the results from experiments carried out on the described robot cell. The kinematics for the two robots where accurately calibrated using the *closed-loop calibration* method described in [25].

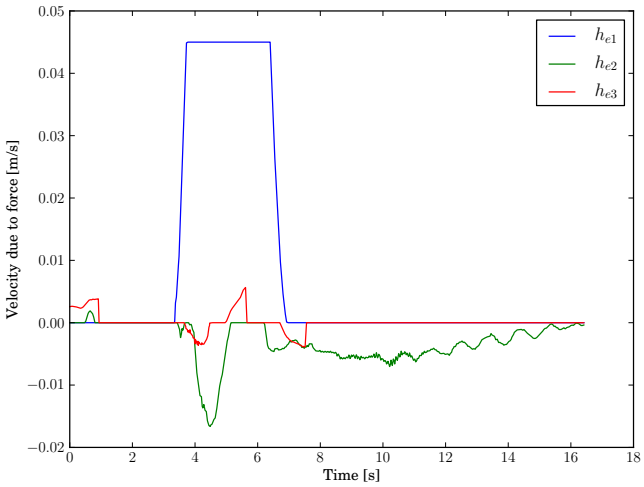

Fig. 4: Twist generated due to external forces.

The object used was a chair seat consisting of a hard plastic shell and a cushion. The weight of the object was about 2.5 kg. The the size of the seat was about 0.5 m across.

The following controller gains and constants were used:

- $k_p = 0.1$
- $k_o = 1$
- $k_{f_p} = 0.005$
- $k_{f_i} = 0.0001$
- $k_{\tau_p} = 0.1$
- $k_{\tau_i} = 0.01$
- $k_{\text{speed down}} = 0.9$
- $k_{\text{speed up}} = 0.999$
- $\mathbf{D} = \text{blockdiag}\ \{\ 0.005\ \mathbf{I}_{3\times3}\ ,\ 0.1\mathbf{I}_{3\times3}\ \}$
- $\epsilon = 0.04$

In addition, the force measurements were linearly filtered using a 1st order low-pass filter with a filter constant of $\alpha_{\text{filter}} = 0.99$. During tuning, which was done by trail and error, it was seen that low-pass filtering of the force measurements was crucial for stability.

The desired object trajectory was implemented as a series of waypoints. A new waypoint is assigned when the previous waypoint is reached within a given tolerance.

Fig. 4 shows the twist due to external forces decomposed in an object-attached coordinate system. It is seen that the applied force, which is largest in the x-direction, reaches its maximum. Fig. 5 shows the position of the object decomposed in the inertial coordinate system. It is seen that before the external interaction, the object moves towards the next waypoint. During the external interaction, after $t = 3.5$ s, the object complies with the force, and moves away from the initial trajectory. After the external interaction ends at $t = 6.5$ s, the object smoothly gains speed towards the waypoint.

The experiment presented here uses full 6-DOF force/motion control, however the external force is mainly applied along one axis. This result in plots which are intuitive, and simple to interpret.

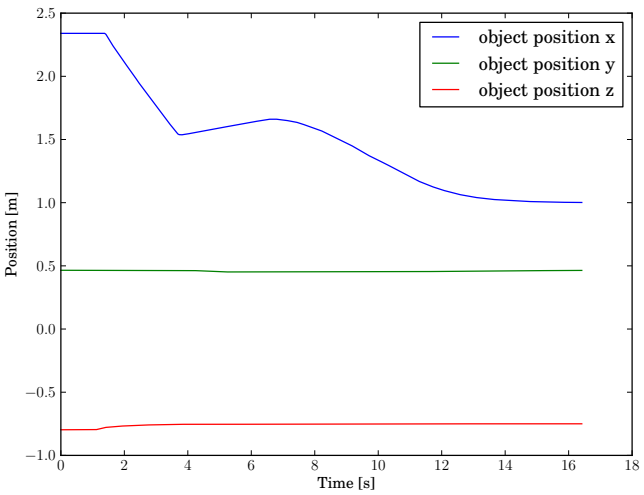

Fig. 5: The position of the object.

A. Experimental Comparison

This section presents a review of experiments in multi-robot handling and manipulations found in the literature. Even though many adaptive and non-adaptive multi-arm handling control schemes have been developed, most papers only report simulation results [6].

Table I presents a detailed list of multi-arm manipulation experiments which are found in the literature. For each experiment, the relevant paper is listed along with the robotic system used in the experiment, as well as control system details and the maximum speed at which motions were carried out. The number of DOF which is reported in the *Robot* column refer to the number of DOF which were used for each robot. The number of DOF in the *experiment* column refer to the DOF for the object. For instance, two robots pushing a box along a plane constitutes a 3-DOF experiment, i.e. position x, y and orientation.

Note that the completeness of this review cannot be guaranteed, but is to the authors knowledge an accurate representation of the state-of-the art within multi-arm manipulation experiments.

It is also seen in the table that the performed experiments often consider few DOF at low speeds. An explanation for this is that many experiments focus on proof-of-concept, rather than performance.

The highest velocity experiment, presented in [13], use small custom-made double pendulums rather than industrial manipulators. In the experiments reported in [26], which are considered high-speed in this context, only 1-DOF is used. Similarly, in [27], the robots are confined to planar motions. Note also that the experiments which consider external force control, such as environmental interaction, are typically executed at low speeds, at the order of mm/s.

The last row in the table describes the experiment presented in this paper. The execution speed is seen to be about four times higher than similar 6-DOF experiment carried out on industrial manipulators.

Ref.	Robot (#)	Type of experiment	Speed
[28]	1-DOF pistons (4)	1-DOF, IF, D, NMB, T.	20 $\frac{\text{mm}}{\text{s}}$
[15]	6-DOF COMAU Smart-3 S, (2)	6-DOF, IF, EF, C, NMB.	2.75 $\frac{\text{mm}}{\text{s}}$
[29]	41-DOF DLR Justin (1)	6-DOF, IF, EF, C, NMB	80 $\frac{\text{mm}}{\text{s}}$
[30]	3-DOF A465 CRS Robotics, (2)	3-DOF, IF, D, MB.	20 $\frac{\text{mm}}{\text{s}}$
[26]	6-DOF Js-2 Kawasaki, (1)	1-DOF, IF, D, NMB.	300 $\frac{\text{mm}}{\text{s}}$
[31]	3-DOF RTX SCARA, (2)	3-DOF, IF, D, MB.	130 $\frac{\text{mm}}{\text{s}}$
[32]	6-DOF PUMA 560, (2)	6-DOF, IF, C, NMB.	100 $\frac{\text{mm}}{\text{s}}$
[33]	3-DOF NA, (2)	1-DOF, IF, D, NMB.	30 $\frac{\text{mm}}{\text{s}}$
[27]	6-DOF PUMA 250, (2)	3-DOF, IF, C, MB.	290 $\frac{\text{mm}}{\text{s}}$
[34]	2-DOF Daikini ltd, (2)	3-DOF, IF, EF, C, MB.	7.7 $\frac{\text{mm}}{\text{s}}$
[13]	2-DOF Custom-made, (2)	3-DOF, IF, D, MB.	600 $\frac{\text{mm}}{\text{s}}$
[35]	4-DOF Aoba Robot System, (2)	4-DOF, IF, C, NMB.	10 $\frac{\text{mm}}{\text{s}}$
[36]	3-DOF Custom-made fingers, (3)	6-DOF, IF, D, MB, T.	25 $\frac{\text{mm}}{\text{s}}$
This paper	7-DOF UR-6-85-5-A, Festo (2).	6-DOF, C, IF, EF, NMB, T.	400 $\frac{\text{mm}}{\text{s}}$

TABLE I: Multi-arm manipulation experiments. EF = External Force control. IF = Internal force control. C=Centralized architecture. D=Decentralized architecture. T=Tracking control. MB/NMB=model-based/non-model-based. (#) indicates the number of robots used in the experiment.

VI. Conclusion and Future Work

A control method for cooperative grasping related to an industrial operation in automated handling of work pieces in a manufacturing cell has been presented. The control method allows for human interaction during cooperative handling. Interaction during motion tracking was achieved using variable admittance control. When external forces are felt, the object becomes compliant. This enabled four times greater execution speeds than for similar experiments reported in the literature.

A demonstrator installation has been built, consisting of two UR-6-85-5-A robots mounted on linear axes with end-effector mounted force/torque sensors. A control platform has been implemented, based on the ROS framework to integrate the sensors and the real-time trajectory generator with the control module.

Experiments have been conducted that demonstrate the feasibility of the proposed control method. The experiments

show considerably faster execution speeds than in similar experiments reported in the literature.

Future work includes adaptive extensions with respect to object mass and center of mass, as well as optimal controller tuning.

ACKNOWLEDGMENTS

This work is part of the project *Next Generation Robotics for Norwegian Industry*, [37]. The project is funded by the Norwegian Research Council and the following end users from the industry: Statoil, Hydro, Tronrud Engineering, Scandinavian Business Seating, Glen Dimplex Nordic and RobotNorge.

The authors also want to thank the SFI Norman program funded by the Research Council of Norway and industrial partners.

REFERENCES

[1] A. Albers, S. Brudniok, J. Ottnad, C. Sauter, and K. Sedchaicharn, "Upper body of a new humanoid robot-the design of armar iii," in *2006 6th IEEE-RAS International Conference on Humanoid Robots*. IEEE, 2006, pp. 308–313.

[2] A. Bicchi, "Hands for dexterous manipulation and robust grasping: A difficult road toward simplicity," *IEEE Transactions on Robotics and Automation*, vol. 16, no. 6, pp. 652–662, 2000.

[3] R. Goertz, "Fundamentals of general-purpose remote manipulators," *Nucleonics*, vol. 10, no. 11, pp. 36–42, 1952.

[4] T. Fletcher, "The undersea mobot," *Report, Nuclear Electronics Laboratory of Hughes Aircraft Company,(6 Jan 1960)*, 1960.

[5] R. O. Ambrose, H. Aldridge, R. S. Askew, R. R. Burridge, W. Bluethmann, M. Diftler, C. Lovchik, D. Magruder, and F. Rehnmark, "Robonaut: Nasa's space humanoid," *Intelligent Systems and their Applications, IEEE*, vol. 15, no. 4, pp. 57–63, 2000.

[6] C. Smith, Y. Karayiannidis, L. Nalpantidis, X. Gratal, P. Qi, D. V. Dimarogonas, and D. Kragic, "Dual arm manipulation: a survey," *Robotics and Autonomous Systems*, 2012.

[7] J. T. Wen and K. Kreutz-Delgado, "Motion and force control of multiple robotic manipulators," *Automatica*, vol. 28, no. 4, pp. 729–743, 1992.

[8] J. Jean and F. Li-Chen, "An adaptive control scheme for coordinated multimanipulator systems," *IEEE Transactions on Robotics and Automation*, vol. 9, no. 2, pp. 226–231, 1993.

[9] A. Rodriguez-Angeles and H. Nijmeijer, "Mutual synchronization of robots via estimated state feedback: a cooperative approach," *IEEE Transactions on Control Systems Technology*, vol. 12, no. 4, pp. 542–554, 2004.

[10] D. Sun and J. Mills, "Adaptive synchronized control for coordination of multirobot assembly tasks," *IEEE Transactions on Robotics and Automation*, vol. 18, no. 4, pp. 498–510, 2002.

[11] W. Gueaieb, F. Karray, and S. Al-Sharhan, "A robust hybrid intelligent position/force control scheme for cooperative manipulators," *Mechatronics, IEEE/ASME Transactions on*, vol. 12, no. 2, pp. 109–125, 2007.

[12] K. Lian, C. Chiu, and P. Liu, "Semi-decentralized adaptive fuzzy control for cooperative multirobot systems with h_∞ motion/internal force tracking performance," *Systems, Man, and Cybernetics, Part B: Cybernetics, IEEE Transactions on*, vol. 32, no. 3, pp. 269–280, 2002.

[13] S. Schneider and J. Cannon, R.H., "Object impedance control for cooperative manipulation: theory and experimental results," *IEEE Transactions on Robotics and Automation*, vol. 8, no. 3, pp. 383–394, 1992.

[14] R. Bonitz and T. C. Hsia, "Internal force-based impedance control for cooperating manipulators," *IEEE Transactions on Robotics and Automation*, vol. 12, no. 1, pp. 78–89, 1996.

[15] F. Caccavale, P. Chiacchio, A. Marino, and L. Villani, "Six-dof impedance control of dual-arm cooperative manipulators," *IEEE/ASME Transactions on Mechatronics*, vol. 13, no. 5, pp. 576–586, 2008.

[16] E. Conkur and R. Buckingham, "Clarifying the definition of redundancy as used in robotics," *Robotica*, vol. 15, no. 5, pp. 583–586, 1997.

[17] M. Spong, S. Hutchinson, and M. Vidyasagar, *Robot modeling and control*. Wiley New Jersey, 2006.

[18] M. Uchiyama and P. Dauchez, "Symmetric kinematic formulation and non-master/slave coordinated control of two-arm robots," *Advanced Robotics*, vol. 7, no. 4, pp. 361–383, 1992.

[19] I. D. Walker, R. Freeman, and S. I. Marcus, "Analysis of motion and internal loading of objects grasped by multiple cooperating manipulators," *The International journal of robotics research*, vol. 10, no. 4, pp. 396–409, 1991.

[20] D. Whitney, "The mathematics of coordinated control of prosthetic arms and manipulators," *Journal of Dynamic Systems, Measurement, and Control*, vol. 94, p. 303, 1972.

[21] J. Yuan, "Closed-loop manipulator control using quaternion feedback," *Robotics and Automation, IEEE Journal of*, vol. 4, no. 4, pp. 434–440, 1988.

[22] B. Siciliano, "Kinematic control of redundant robot manipulators: A tutorial," *Journal of Intelligent and Robotic Systems*, vol. 3, no. 3, pp. 201–212, 1990.

[23] J. Schrimpf, M. Lind, A. Skavhaug, and G. Mathisen, "Implementation details of external trajectory generation for industrialrobots." in *Proceedings of IWAMA 2012 - The Second International Workshop of Advanced Manufacturing and Automation*, 2012.

[24] J. Schrimpf, M. Lind, and G. Mathisen, "Real-time analysis of a multi-robot sewing cell," in *IEEE International Conference on Industrial Technology (ICIT)*, february 2013.

[25] R. Bonitz and T. Hsia, "Calibrating a multi-manipulator robotic system," *Robotics Automation Magazine, IEEE*, vol. 4, no. 1, pp. 18–22, 1997.

[26] Y. Maeda, T. Hara, and T. Arai, "Human-robot cooperative manipulation with motion estimation," in *IEEE/RSJ International Conference on Intelligent Robots and Systems*, vol. 4. IEEE, 2001, pp. 2240–2245.

[27] E. Paljug, X. Yun, and V. Kumar, "Control of rolling contacts in multi-arm manipulation," *IEEE Transactions on Robotics and Automation*, vol. 10, no. 4, pp. 441–452, 1994.

[28] R. Bacocco, G. Borghesan, and C. Melchiorri, "Experimental evaluation of two control schemes for cooperative teleoperation," in *World Automation Congress (WAC)*. IEEE, 2012, pp. 1–6.

[29] T. Wimbock, C. Ott, and G. Hirzinger, "Impedance behaviors for two-handed manipulation: Design and experiments," in *IEEE International Conference on Robotics and Automation*. IEEE, 2007, pp. 4182–4189.

[30] J. Gudiño-Lau and M. A. Arteaga, "Dynamic model and simulation of cooperative robots: a case study," *Robotica*, vol. 23, no. 5, pp. 615–624, 2005.

[31] J. Wang, S. Dodds, and W. N. Bailey, "Co-ordinated control of multiple robotic manipulators handling a common object-theory and experiments," *IEEE Proceedings Control Theory and Applications*, vol. 144, no. 1, pp. 73–86, 1997.

[32] R. Bonitz and T. Hsia, "Robust dual-arm manipulation of rigid objects via palm grasping-theory and experiments," in *IEEE International Conference on Robotics and Automation*, vol. 4, 1996, pp. 3047–3054 vol.4.

[33] T. Mukaiyama, K. Kim, and Y. Hori, "Implementation of cooperative manipulation using decentralized robust position/force control," in *4th International Workshop on Advanced Motion Control. (AMC)*, vol. 2, 1996, pp. 529–534 vol.2.

[34] T. Yoshikawa and X.-Z. Zheng, "Coordinated dynamic hybrid position/force control for multiple robot manipulators handling one constrained object," *The International Journal of Robotics Research*, vol. 12, no. 3, pp. 219–230, 1993.

[35] M. Uchiyama, N. Iwasawa, and K. Hakomori, "Hybrid position/force control for coordination of a two-arm robot," in *IEEE International Conference on Robotics and Automation.*, vol. 4, 1987, pp. 1242–1247.

[36] S. Arimoto, F. Miyazaki, and S. Kawamura, "Cooperative motion control of multiple robot arms or fingers," in *IEEE International Conference on Robotics and Automation.*, vol. 4. IEEE, 1987, pp. 1407–1412.

[37] I. Schjølberg, "Development of robot solutions for oil/ gas, aluminium and manufacturing industry," *17th IEEE Conference on Emerging Technologies and Factory Automation (EFTA), Krakow, Poland*, vol. 5, no. 1, p. 90, 2012.